


# Quantum chemical study of heterocyclic organic compounds on the corrosion inhibition

Dyari Mustafa Mamand<sup>a</sup>, Awat Hamad Awla<sup>a</sup>,  
Twana Mohammed Kak Anwer<sup>b</sup>, Hiwa Mohammad Qadr<sup>a\*</sup> 

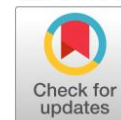
a: Department of Physics, College of Science, University of Raparin, 46012 Sulaymaniyah, Iraq

b: Department of Physics, College of Science Education, Salahaddin University, Erbil, Iraq

\* Corresponding author: [hiwa.physics@uor.edu.krd](mailto:hiwa.physics@uor.edu.krd)

This paper belongs to a Regular Issue.

© 2021, the Authors. This article is published open access under the terms and conditions of the Creative Commons Attribution (CC BY) license (<http://creativecommons.org/licenses/by/4.0/>).



## Abstract

Corrosion damages all materials, necessitating replacement and inspection related expenses. Thus, the demand has increased for new corrosion inhibitor materials. The ratios of corrosion inhibition of materials are different, but organic compounds have high efficiency in aqueous corrosion inhibition for various alloys and metals. This efficiency can increase in the presence of O, N and S. The molecule provides great inhibition with the presence of both S and N atoms in the same compound. This paper investigates the 1, 3, 4-thiadiazole molecule and electronic structure of several organic compounds such as  $R_1$  and  $R_2$  which consist of different substituent groups. They were united to the ring of 1, 3, 4-thiadiazole to provide nine different derivatives. Quantum computations (density functional theory, DFT) at 6-311G++ ( $d$ ,  $p$ ) basis set and Becke's three parameters hybrid (B3LYP) level were performed using Gaussian program. The purpose of this study is to determine the chemical behaviour of several heterocyclic organic compounds and to understand the process of the corrosion inhibition.

## Keywords

DFT  
HUMO  
LUMO  
corrosion inhibition  
1, 3, 4-thiadiazole

Received: 25.10.21

Revised: 07.04.22

Accepted: 09.04.22

Available online: 17.04.22

## 1. Introduction

Corrosion is the degradation of the material and it is generally a slow process [1]. But it can accelerate if incompatible materials are combined, e.g. when two materials with different electrochemical activity are in electrical contact with each other. In this process, more passive metal drives the corrosion of the active metal at the same time as the passive metal remains unharmed [2-4]. This process keeps going until the active metal has been completely gone or the electrical connections between the two metals have been broken. Using corrosion inhibitors is one of the best and most effective ways to protect the surface of materials from corrosion in acid environments [5]. Watery corrosion of metallic surfaces can be hindered with organic materials [6]. Nowadays, these compounds have a good capability for the prevention of metallic surface abuse, which has caused their widespread usage [7]. Decreasing the cathode reaction with the anodic process of destruction of the mineral in acid solution, these factors all stem from the inhibitors adsorbed on the surface of the met-

als [8]. This leads to the creation of a diffusion barrier between two sides. The electrical conductivity is drastically decreased due to forming a diffusion barrier that surrounds the reaction sites [9]. There are many ways to prevent metallic material from corrosion. Some materials, such as those containing heteroatoms, are beneficial for preventing corrosion. Organic compounds containing  $\pi$  bonds and N, O, S have been widely used [10].

In previous years, theoretical methods have been widely used in various fields [11]. Quantum computational method is realized in the Gaussian Program [12]. A theoretical calculations in the Gaussian Program can be used to estimate corrosion inhibition performances of molecules [13]. The corrosion inhibition efficiencies are determined by the experimental method and allowed to estimate the corrosion inhibition mechanisms of composites in terms of weight loss [14]. Nitrogen and sulfur are two important atoms for inhibition. It would be beneficial, if the two of them came together in the same molecule [14]. However, if the compounds consist of oxygen or nitrogen, the effect will be reduced. So, it will not provide an excellent inhibition [15]. The ability of these compounds to inhibit corro-

sion depends on the structure of the molecular [16]. The adsorption of these molecules on metallic surfaces is important in this regard, and it is possible to estimate it, as it depends on the lone electron pairs in the heteroatoms [17]. The computational method in quantum chemistry is able to predict some parameters such as hardness and softness [18, 19].

This paper investigates the molecular structure and electronic behaviour of some organic compounds by using quantum computational method based on DFT. Hardness, softness, electronegativity and chemical potential are important parameters for quantum chemical method.

## 2. Computational Details

Density functional theory (DFT) is a computational quantum mechanical modelling method used in this study to calculate the electronic structure of atoms and molecules [20]. The quantum chemical calculations based on DFT at 6-311G++ (*d, p*) basis set were used because this basis set is very popular for determining the electronic and molecular geometry accurately. All computations were performed with Gaussian 09 package program. The 6-311G is the standard, split-valence and double-zeta basis set use to describe the core and valence orbitals, (*d, p*) are polarization function to describe the chemical bonds and ++ are diffuse functions [21]. 6-311G++ (*d, p*) basis set is very useful and can accurately calculate high occupied molecular orbital (HOMO), lower unoccupied molecular orbital (LUMO), hardness, softness, electronegativity, chemical reaction, electrophilicity, proton affinity and nucleophilicity [22]. The use of Fukui indices can predict the local molecular reactivity [23]. The Fukui function  $f(\vec{r})$  can be written with the following expression [24]:

$$f(\vec{r}) = \left( \frac{\rho(\vec{r})}{\partial N} \right)_{v(\vec{r})}, \quad (1)$$

where  $\rho$  is the electronic density of the system under consideration,  $N$  is the number of electrons and  $v(\vec{r})$  is the external potential.

Removal or addition of an electron in the relaxation effects is not measured approximately from the Fukui function. The removal and addition of an electron can be expressed as follows:

$$\rho^-(\vec{r}) \approx \rho_{LUMO}(\vec{r}), \quad (2)$$

$$\rho^+(\vec{r}) \approx \rho_{HOMO}(\vec{r}), \quad (3)$$

where  $\rho_{LUMO}(\vec{r})$  is the density for the lowest unoccupied molecular orbital and  $\rho_{HOMO}(\vec{r})$  is the density of the highest occupied molecular orbital [25]. Condensed Fukui functions are used for the local activity sites which are determined by using the infinitesimal change, limited variation and approximations of quantum computational

chemistry from the Mulliken population analysis of atoms, which depend on the direction of electron transfer of atoms in molecules [26]. There are two types of local active sites - the nucleophilic and the electrophilic. In the nucleophile site, the electrons will transfer from the nucleophile to the electrophile. But, in the electrophile site, the electron will transfer to the end site of electrophile [27]. Each of  $R_1$  and  $R_2$  consist of different substituent groups, which are united to the ring of 1, 3, 4-thiadiazole to provide nine various derivatives as shown in Figure 1, where  $R_1$  consists of (H), hydrogen, and (-CH<sub>3</sub>), methyl, while  $R_2$  consists of a variety of substituents united to 1, 3, 4-thiadiazole. The substituent groups consist of ethyl (-C<sub>2</sub>H<sub>5</sub>), methyl (-CH<sub>3</sub>), propyl (-C<sub>3</sub>H<sub>7</sub>), chloroethyl (-C<sub>2</sub>H<sub>5</sub>-Cl), hydroxyethyl (-C<sub>2</sub>H<sub>5</sub>-OH), tioethyl (-C<sub>2</sub>H<sub>5</sub>-SH), carboxyethyl (-C<sub>2</sub>H<sub>5</sub>-COOH) and aminoethyl (-C<sub>2</sub>H<sub>5</sub>-NH<sub>2</sub>). Figure 2 shows the chemical structure of 1, 3, 4-thiadiazole derivatives 1-9.

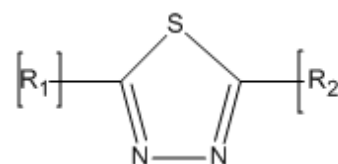


**Figure 1** Chemical structure of 1, 3, 4-thiadiazole ring with  $R_1$  and  $R_2$  substituents.

## 3. Computational Results

Quantum computational chemistry method optimized geometries of the compounds with nine various substitutions of the ring (1, 3, 4-thiadiazole) by using Gaussian program with 6-311G++ (*d, p*) basis set as shown in Figure 2 [28, 29]. The structures of these derivatives are presented in Figure 3: (1) 2-methyl-1,3,4-thiadiazole (2) 2-propyl-5-methyl-1,3,4-thiadiazole (3) 2,5-dimethyl-1,3,4-thiadiazole; (4) 2-ethyl-5-methyl-1,3,4-thiadiazole (5) 2-(2-hydroxyethyl)-5-methyl-1,3,4-thiadiazole; (6) 2-aminoethyl-5-methyl-1,3,4-thiadiazole; (7) 2-(2-chloroethyl)-5-methyl-1,3,4-thiadiazole; (8) 2-(2-carboxy ethyl)-5-methyl-1,3,4-thiadiazole; and (9) 2-(2-tioethyl)-5-methyl-1,3,4-thiadiazole.

## 4. Quantum chemical calculations

HOMO, LUMO and frontier orbital gap are significant parameters in quantum computational chemistry. They are important for the kinetic stability and chemical reactivity of the molecules [30, 31]. Table 1 shows the bandgap energies of nine different derivatives. The charge-transfer interaction inside the molecule is explained by the energy gap of HOMO and LUMO [32]. They are two popular parameters in quantum chemistry. Frontier orbitals are the main factors to describe the molecule's interaction with other species.

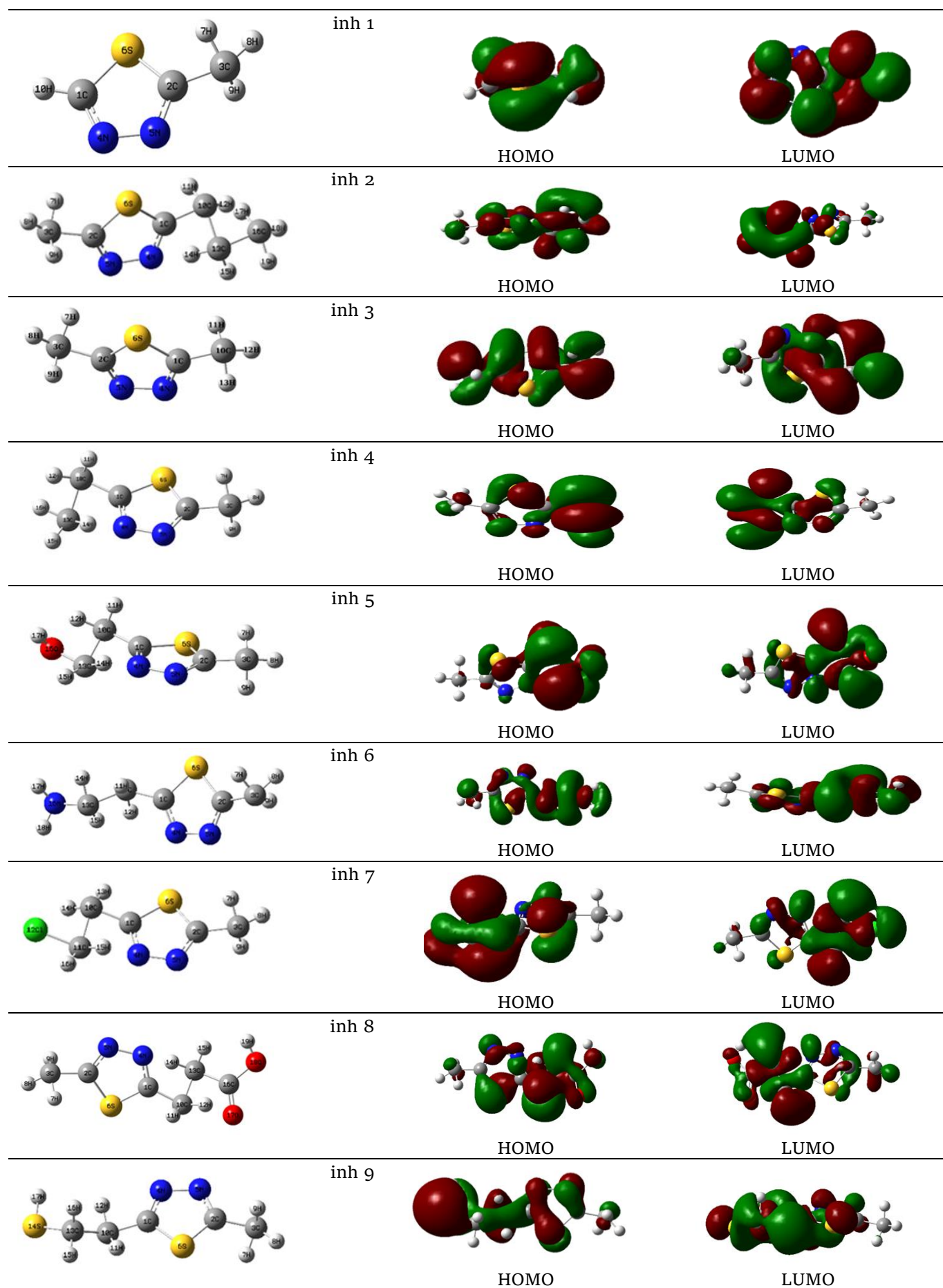


**Figure 2** The optimized structures of LUMO and HOMO using DFT/B3LYP/6-31++G (d, p) of non-protonated inhibitor molecules 1 to 9 in gas phase.

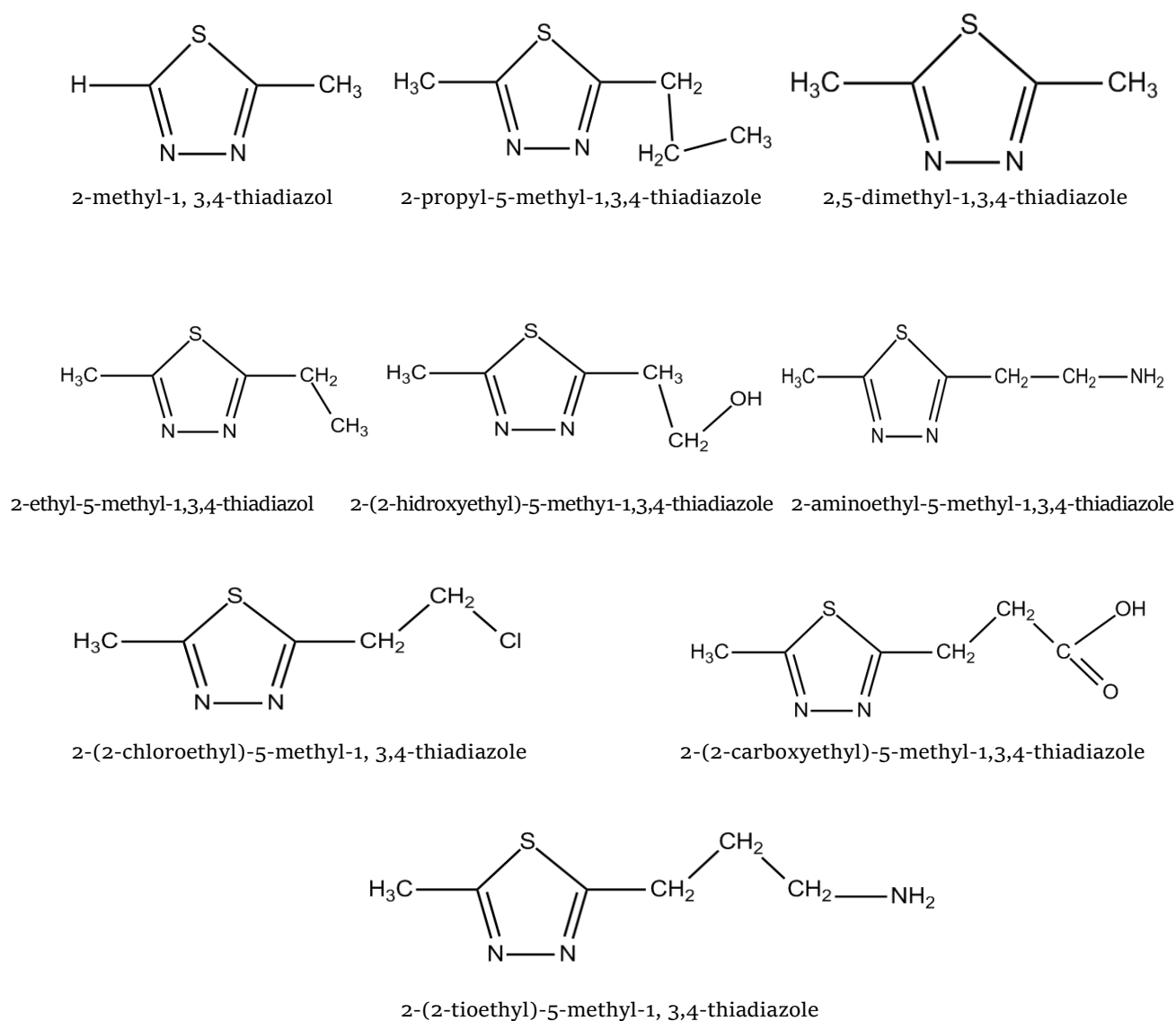


**Figure 3** Chemical structure of 1, 3, 4-thiadiazole derivatives 1-9.

The chemical interaction between HOMO and LUMO decides the formation of transition states [33]. The ability of molecules to donate electrons can be found with the energy of  $E_{\text{HOMO}}$  [34]. The tendency to donate electrons in the molecules is related to the energy of  $E_{\text{HOMO}}$  [35]. If the molecule has a high  $E_{\text{HOMO}}$ , the tendency to donate an electron will increase to allow acceptor molecules with low energy and empty molecular orbital. Facile adsorption of molecules (i.e. the inhibition) will increase with the increase in the value of  $E_{\text{HOMO}}$  due to adsorbed layer which influences the transportation process [36]. The probability of accepting electrons by the molecules is related to the value of  $E_{\text{LUMO}}$ , the tendency of accepting electrons by molecules will increase with the lower value of  $E_{\text{LUMO}}$ . Materials have a good inhibition efficiency if they have lower bandgap energy. In this case, more energy is required to transfer the electron from the last lowest occupied orbital and the surface of the material [37]. In recent years, quantum chemical approaches have shown to be particularly beneficial in the assessment of prospective corrosion inhibitors. Quantum chemical parameters based on the DFT,

such as chemical potential, chemical hardness, electrophilicity, electronegativity, and nucleophilicity, have been used to investigate the results of the computational chemistry works' consistency with experimental data [38]. Indeed, Koopmans theorem is one of the most significant contributions to the computational chemistry research. Following that, it is possible to explain hard and soft acid-base (HSAB) theory in detail. Pearson developed the HSAB theory as a result of studies on Lewis acid bases in the 1960 [39]. Bases and Lewis acids were characterized as hard or soft, based on this hypothesis. The hard acids choose to correlate with hard bases, but soft acids prefer to associate with soft bases. The description for these purposes is that the soft-soft interactions are frequently covalent, but hard-hard interactions are electrostatic. Because the corrosion inhibitors are Lewis bases, the HSAB theory should be included in corrosion research [13]. Furthermore, the HSAB theory is a significant advancement in quantum chemistry, which is useful in a variety of theoretical and experimental research involving corrosion inhibitors, chemical equilibrium, complex stability, precipitation

titrations and gravimetry. The chemical potential ( $\mu$ ), chemical hardness ( $\eta$ ) and reactivity indexes electronegativity ( $\chi$ ) are described as derivatives of the number of electrons ( $N$ ) of the electron energy ( $E$ ) at external potential ( $v$ ) in the conceptual DFT. The expression for the mathematical operations can be obtained as:

$$I = -E_{HOMO}, \quad (4)$$

$$A = -E_{LUMO}, \quad (5)$$

$$\chi = \left(\frac{I + A}{2}\right), \quad (6)$$

$$\eta = \left(\frac{I - A}{2}\right), \quad (7)$$

$$\sigma = \frac{1}{\eta}, \quad (8)$$

$$\omega = \frac{\mu^2}{2\eta}, \quad (9)$$

where  $I$  is the ionization energy,  $A$  is the electron affinity,  $\sigma$  is the softness and  $\omega$  is the electrophilicity.

## 5. Mulliken atomic charges and Fukui function calculations in the gas phase

The value of bandgap energy of each derivative reduces, evidencing the increase of corrosion inhibition of 1, 3, 4-thiadiazole with substituents. The hardness and softness of molecules are related to  $E_{LUMO}$  and  $E_{HOMO}$ . Reactivity towards chemical species depends on the bandgap energy, where high reactivity towards chemical species indicates a small bandgap [40]. A hard molecule has lower reactivity than a soft molecule because a soft molecule has a small bandgap energy [41]. Reactivity and stability of molecules are two parameters that can be determined by measuring the softness and hardness properties of molecules [42, 43]. The harness properties of the materials in a low perturbation of the reactions are the resistance to prevent deformation, preventing the polarization of the electron cloud of the molecules. Inhibition properties of the molecules will rise with an increase in the value of softness.

Inhibition efficiency will be highest when the softness is the highest, which is in agreement with our conclusions [44].

All calculations were performed with quantum computational chemistry for the derivatives of 1, 3, 4-thiadiazole in the gas phase, as shown in Tables 1 and 2. For each of derivatives of 1, 3, 4-thiadiazole molecule, Fukui indices have been calculated. Tables 1 and 2 are expressed in terms of ionization energy, where  $\Delta E$ ,  $CP$  and  $\varepsilon$  are the energy gap, the chemical potential and the nucleophilicity.

Table 1 shows the calculated values of  $E_{HOMO}$  and  $E_{LUMO}$  for the investigated derivatives 1–9 in non-protonated gas. The order of inhibition efficiency of the investigated inhibitors corresponds to the order established from theoretical data based on  $E_{HOMO}$ , which is  $1 < 9 < 8 < 3 < 4 < 5 < 6 < 7 < 2$ . However, based on the results obtained for  $E_{LUMO}$  in the gas phase, the value of  $E_{LUMO}$  changes follows:  $1 > 9 > 8 > 3 > 4 > 5 > 6 > 7 > 2$ . As a function of the reaction of the inhibitor molecule towards adsorption on the metal surface, the energy gap is an important descriptor. The reactivity of the molecule increases due to the reduction of  $\Delta E$ . It is known that corrosion inhibitors with small energy gaps are effective because the ionization energy needed to remove the electron from the final occupied orbital is low. according to Bereket et al., organic compounds do not only donate electrons to empty metal orbitals, but also accept free electrons from metals [45]. Furthermore, a molecule with a lower energy gap appears to be more polarizable and typically characterized by low kinetic stability and strong chemical activity. The results in Table 1 shown that inhibitor 1 has the smallest energy gap under all conditions, which means the molecule can perform better as a corrosion inhibitor.

Absolute hardness and softness are well-known qualities to determine molecule stability and reactivity. According to Obi-Egbedi, chemical hardness is defined as the resistance to deformation or polarization of the electron cloud of atoms, ions, or molecules under minor perturbations of chemical reactions [46]. A soft molecule has a tiny energy gap, whereas a hard molecule has a big energy gap. As a result, molecules in the lowest global hardness values are supposed to be effective corrosion inhibitors for bulk metals in acidic environments.

**Table 1** Gas phase calculations with 6-311++(d, p) basis set and B3LYP level for molecular characteristics of compounds 1–9.

No.	HOMO (eV)	LUMO (eV)	$I$	$A$	$\Delta E$ (eV)	$\eta$	$\sigma$	$\chi$	$CP$	$\omega$	$\varepsilon$
1	-6.2861	-2.1850	6.28615	2.18509	4.1010	2.05053	0.48767	4.235	-4.235628	4.3745	0.22859
2	-6.8684	-6.4850	6.86847	6.48506	0.3834	0.19170	5.21632	6.676	-6.6767	116.27	0.00860
3	-7.1555	-3.5951	7.15556	3.59519	3.5603	1.78018	0.56174	5.375	-5.37537	8.1156	0.12321
4	-7.5808	-5.5582	7.58087	5.55824	2.0226	1.01131	0.98880	6.569	-6.56956	21.338	0.04686
5	-7.1955	-6.1615	7.19556	6.16152	1.0340	0.51702	1.93415	6.678	-6.6785	43.134	0.02318
6	-7.3011	-6.3490	7.30114	6.34901	0.9521	0.47606	2.10054	6.825	-6.8250	48.923	0.02044
7	-6.4091	-5.6156	6.40914	5.61565	0.7934	0.39674	2.52050	6.012	-6.01240	45.556	0.02195
8	-7.5982	-5.1299	7.59829	5.12993	2.4683	1.23418	0.81025	6.364	-6.36411	16.408	0.06094
9	-6.6184	-3.9364	6.61840	3.93643	2.6819	1.34098	0.74571	5.277	-5.27741	10.384	0.09629

**Table 2** Gas phase calculations of Fukui functions and Mulliken atomic charges at 6-311G++ (*d, p*) basis set at B3LYP level for derivatives 1–9.

No.	Atoms	$q_N$	$q_{N+1}$	$q_{N-1}$	$f_k^+$	$f_k^-$	$f_k^0$
1	N4	-0.106	-0.030	-0.130	0.076	0.024	0.050
	N5	0.065	0.166	-0.034	0.101	0.099	0.100
	S6	0.082	0.228	-0.124	0.146	0.206	0.176
2	N4	0.025	0.061	0.011	0.036	0.014	0.025
	N5	-0.315	-0.215	-0.329	0.100	0.014	0.057
	S6	0.235	0.349	0.209	0.114	0.026	0.070
3	N4	-0.227	-0.148	-0.254	0.079	0.027	0.053
	N5	-0.296	-0.218	-0.299	0.078	0.003	0.0405
	S6	0.402	1.035	0.332	0.633	0.070	0.3515
4	N4	0.034	0.039	0.008	0.005	0.026	0.0155
	N5	-0.354	-0.317	-0.362	0.037	0.008	0.0225
	S6	0.266	0.359	0.235	0.093	0.031	0.062
5	N4	0.070	0.075	0.016	0.005	0.054	0.0295
	N5	-0.303	-0.294	-0.312	0.009	0.009	0.009
	S6	0.194	0.226	0.179	0.032	0.015	0.0235
	O16	-0.353	-0.307	-0.365	0.046	0.012	0.029
	N4	0.070	0.075	0.016	0.005	0.054	0.0295
6	N4	-0.144	-0.129	-0.181	0.015	0.037	0.026
	N5	-0.318	-0.297	-0.331	0.021	0.013	0.017
	S6	0.309	0.396	0.290	0.087	0.019	0.053
	N16	-0.378	-0.290	-0.479	0.088	0.101	0.0945
7	N4	0.056	0.058	-0.012	0.002	0.068	0.035
	N5	-0.237	-0.230	-0.240	0.007	0.003	0.005
	S6	0.116	0.200	0.109	0.084	0.007	0.0455
	Cl12	0.764	0.822	0.639	0.058	0.125	0.0915
8	N4	-0.016	-0.011	-0.066	0.005	0.05	0.0275
	N5	-0.250	-0.211	-0.256	0.039	0.006	0.0225
	S6	0.195	0.298	0.181	0.103	0.014	0.0585
9	N4	-0.193	-0.191	-0.239	0.002	0.046	0.0240
	N5	-0.356	-0.321	-0.365	0.035	0.009	0.0220
	S6	0.253	0.286	0.213	0.033	0.040	0.0365

Inhibitor adsorption occurs on a metal surface in the softest part of the molecule. Table 1 shows the calculated values of the gas phases for the analysed derivatives 1–9. Compared with other inhibitors, 1, 3, 9 and 8 have the highest levels of hardness. Compared with the derivatives, the data for B3LYP/6-311++G (*d, p*) show that inhibitor 1 has the highest stiffness value of 2.05 eV in the non-protonated gas phase.

Table 2 shows the gas phase calculations of Fukui functions and Mulliken atomic charges at 6-311G++ (*d, p*) basis set at B3LYP level for derivatives 1–9, where  $f_k^+$ ,  $f_k^-$  and  $f_k^0$  are the nucleophilic attack, the electrophilic attack and the radical attack. A high value of the nucleophilic attack site indicates the increased ability of the molecules to accept electrons, and the molecule will be more able to stabilize additional electrons [47]. The tendency of a molecule to donate electrons is defined by the high electrophilic site value. The ability of the metal surface to donate electrons increases with an increase in the inhibition efficiency [40]. Figure 3 shows the optimized structures LUMO and HOMO using DFT/B3LYP/6-311++G (*d, p*) of non-protonated inhibitor molecules 1–9.

## 6. Mulliken atomic charges and Fukui function for derivatives 1–9 in the presence of water

Only four atoms O, N, S, and Cl were shown in Mulliken charge and Fukui function calculations to determine the effect of each of the atoms on the molecule because of the existence of electrochemical corrosion in the liquid phase. It is obvious that quantum computational calculations in the aqueous phase are necessary to show the effect of solvents on corrosion inhibition of organic compounds. For this purpose, Gaussian program can describe the properties of organic compounds. In this case, the polarized continuum method PCM was used [48]. The solute is placed in a cavity of a roughly molecular shape. For determining the effect of solvent on geometry optimization calculations, the solvent in these models is defined by a continuum that interacts with charges on the cavity surface [49]. Table 3 shows the aqueous phase calculations with 6-311++ (*d, p*) basis set and B3LYP level for molecular characteristics of the compounds 1–9. Table 4 shows the aqueous phase calculations of Fukui functions and Mulliken atomic charges at 6-311G++ (*d, p*) basis set at B3LYP level for the derivatives 1–9.

**Table 3** Aqueous phase calculations with 6-311++ (*d, p*) basis set and B3LYP level for molecular characteristics of compounds 1–9.

No.	HOMO (eV)	LUMO (eV)	I	A	$\Delta E$ (eV)	$\eta$	$\sigma$	$\chi$	CP	$\omega$	$\epsilon$
1	-8.26307	-4.0488	8.26307	4.04881	4.21426	2.10713	0.47457	6.15594	-6.1559	8.992	0.11120
2	-7.59611	-7.1969	7.59611	7.19692	0.39919	0.19959	5.01009	7.39652	-7.3965	137.04	0.00729
3	-7.23093	-5.7757	7.23093	5.77579	1.45514	0.72757	1.37443	6.50336	-6.5033	29.065	0.03440
4	-6.82249	-4.9440	6.8224	4.94407	1.87841	0.93920	1.06472	5.88328	-5.8832	18.426	0.05426
5	-6.44425	-5.4951	6.4442	5.49511	0.94914	0.47457	2.10716	5.96968	-5.9696	37.546	0.02663
6	-6.59527	-5.5862	6.59527	5.58626	1.00900	0.50450	1.98214	6.09077	-6.0907	36.766	0.02719
7	-6.40914	-5.6156	6.4091	5.6156	0.7934	0.3967	2.5205	6.01240	-6.0124	45.556	0.02195
8	-6.81324	-4.4303	6.8132	4.4303	2.3829	1.1914	0.8393	5.6217	-5.6217	13.262	0.07539
9	-6.61840	-3.9364	6.6184	3.9364	2.6819	1.3409	0.7457	5.2774	-5.2774	10.384	0.09629

**Table 4** Aqueous phase calculations of Fukui functions and Mulliken atomic charges at 6-311G++ (*d, p*) basis set at B3LYP level for derivatives 1–9.

No.	Atoms	$q_N$	$q_{N+1}$	$q_{N-1}$	$f_k^+$	$f_k^-$	$f_k^0$
1	N4	-0.288	-0.114	-0.333	0.174	0.045	0.1095
	N5	-0.219	-0.205	-0.238	0.014	0.019	0.0165
	S6	0.633	1.189	0.575	0.556	0.058	0.307
2	N4	0.033	0.061	0.011	0.028	0.022	0.025
	N5	-0.212	-0.215	-0.329	-0.003	0.117	0.057
	S6	0.248	0.349	0.209	0.101	0.039	0.07
3	N4	-0.511	-0.441	-0.535	0.07	0.024	0.047
	N5	-0.519	-0.430	-0.535	0.089	0.016	0.0525
	S6	0.804	1.450	0.761	0.646	0.043	0.3445
4	N4	0.034	0.039	0.008	0.005	0.026	0.0155
	N5	-0.354	-0.317	-0.362	0.037	0.008	0.0225
	S6	0.266	0.359	0.235	0.093	0.031	0.062
5	N4	0.070	0.075	0.016	0.005	0.054	0.0295
	N5	-0.303	-0.294	-0.312	0.009	0.009	0.009
	S6	0.194	0.226	0.179	0.032	0.015	0.0235
6	O16	-0.353	-0.307	-0.365	0.046	0.012	0.029
	N4	-0.144	-0.129	-0.331	0.015	0.187	0.101
	N5	-0.318	-0.297	-0.181	0.021	-0.137	-0.058
7	S6	0.309	0.369	0.290	0.06	0.019	0.0395
	N16	-0.378	-0.290	-0.479	0.088	0.101	0.0945
	N4	0.056	0.058	-0.012	0.002	0.068	0.035
8	N5	-0.237	-0.230	-0.240	0.007	0.003	0.005
	S6	0.116	0.200	0.109	0.084	0.007	0.0455
	Cl12	0.764	0.822	0.639	0.058	0.125	0.0915
9	N4	-0.016	-0.011	-0.066	0.005	0.05	0.0275
	N5	-0.250	-0.211	-0.256	0.039	0.006	0.0225
	S6	-0.195	0.298	0.181	0.493	-0.376	0.0585
9	N4	-0.193	-0.191	-0.239	0.002	0.046	0.024
	N5	-0.356	-0.321	-0.365	0.035	0.009	0.022
	S6	0.253	0.286	0.213	0.033	0.04	0.0365

The bond distance from the analyses of the optimized geometry at 6-311++G (*d, p*) basis set between C2 and R2 remained unchanged and equal to 1.54 Å. The bond angle of the 1, 3, 4-thiadiazole internal ring for S6–C2–N4 and S6–C2–N4 is 111.10865–111.108660, respectively. At the first derivative, the difference between them is very small, but at the second derivative it is 0.006°. The bond angle between C1–N4 and C2–N4 is in the same range for all derivatives, about 1.34983° and 1.34982°. The bond length between C1–N4 and C2–N4 shows just small variations. For this purpose, it is reasonable to arrange all the derivatives which showed a length of C1–N4 and C2–N4 bond of 1.34 Å. The bond angle between S6–C1 and S6–C2 is 1.75805° for each of the optimized geometry calculations, indicating the formation of single bonds between these atoms.

N4, N5, S6, O16 and Cl12 have a high electronic density, which was calculated by Mulliken population analysis for each derivative. Due to the high electronic density, these atoms are nucleophilic when they interact with the metallic surface. The HOMO calculations in the presence of solvents (water) are shown in Figure 3. In all compounds, HOMO is placed on both sides of the functional groups attached to the 1, 3, 4-thiadiazole ring. This calculation shows the positions of the approved active sites for an electrophilic attack. The active region is distributed around the molecule belonging to the 1, 3, 4-thiadiazole ring.

The inhibitor with the lowest global hardness (and thus the highest global softness) is likely to have the best inhibition efficiency. The following anticorrosion efficiency was predicted in our study: the inhibitor 2 is more efficient than the inhibitor 7, 5 – than 6, 9 – than 1. According

to Hasanov et al., adsorption can occur in the part of the molecule where softness is at maximum [50].

An electrophile is a chemical species that accepts a pair of electrons. The molecule with the larger electrophilicity value has the greater ability to receive electrons, and its opposite will behave as a good nucleophile. Tables 1 and 2 shows the compounds with low electrophilic values (good nucleophiles). Table 3 shows both the electrophilic and nucleophilic data. The corrosion inhibition efficiency rating of the investigated compounds can be defined as follows:  $1 < 9 < 8 < 4 < 3 < 6 < 5 < 7 < 2$ .

When electronegativity and chemical potentials are equal, electrons flow from the lower-electronegative site to the higher as the inhibitor and iron come close to each other. The fraction of electrons transferred can be calculated from the following equation:

$$\Delta N_{max} = \frac{\chi_{Fe} - \chi_{inh}}{2(\eta_{Fe} - \eta_{inh})} \quad (10)$$

The electronegativity of the inhibitor and the metal are represented by  $\chi_{Fe}$  and  $\chi_{inh}$ . The chemical hardness of the inhibitor is  $\eta_{inh}$  and that of the metal -  $\eta_{Fe}$ . Pearson has been demonstrated that electron transfer is driven by electronegativity differences and the aggregation of  $\eta$  factors acts as a barrier [51]. As a result, the electronegativity of Fe = 7 eV and a global  $\eta$  of Fe = 0 were used to calculate the ratio of electrons transferred assuming that for the metallic mass  $I$  is equal to  $A$  because it is softer than the neutral metal atoms [52]. Tables 5 and 6 shows quantum chemical parameters of derivatives 1-9 in the gas and aqueous phases with 6-311++ ( $d, p$ ) basis set and B3LYP level. The positive number  $\Delta N_{max}$  indicates that the molecules are electron acceptors, while the negative number of  $\Delta N_{max}$  indicates that the molecules are electron donors. As a result of that as the electron-donating capacity of these inhibitors increases on the metal surface, the inhibition efficiency also increases. Moreover, as the electron-donating ability at the metal surface increases, the inhibition efficiency also increases if  $\Delta N_{max} < 3.6$ . The inhibitor molecules' capacity to accept electrons changes in the sequence  $7 > 2 > 1 > 9 > 3 > 5 > 8 > 4 > 6$  in the gas phase and in the aqueous phase - as follows:  $7 > 8 > 9 > 6 > 4 > 8 > 3 > 1 > 2$ . The inhibitor 2 is a donor compound in the aqueous phase. Figure 5 shows the optimized structures, HOMOs of non-protonated inhibitor molecules using DFT/B3LYP/6-31++G ( $d, p$ ) in the aqueous phase.

A study by Gomez et al. postulated that an electronic back-donation mechanism can control the interaction between the metal surface and the inhibitor molecule, based on the charge transfer model for back-donation and donation of charges [53, 54]. According to this theory, if back-donation transfers from the molecule and electron to the molecule at the same time, the energy change  $\Delta E_{b-d}$  is proportional to the molecule's hardness. That is,

$$\Delta E_{b-d} = -\frac{\eta}{4} \quad (11)$$

From the molecule to the metal, the back donation is strongly preferred when  $\eta > 0$  or  $\Delta E_{b-d} < 0$ . It indicates that charge transfer to the molecule is accompanied by the back donation from the molecule, which is energetically beneficial on the metal surface, if the higher adsorption of the molecule enhances inhibition effectiveness. Then, the inhibition efficiency should arise with the increase in the stabilization energy induced by the contact between the inhibitor and the metal surface. In this study, the calculated  $\Delta E_{b-d}$  values exhibit the tendency:  $2 > 7 > 5 > 6 > 4 > 8 > 9 > 3 > 1$  in the gas phase, and in the aqueous phase the tendency is:  $2 > 7 > 5 > 6 > 3 > 4 > 8 > 9 > 1$ , as shown in Tables 5, 6.

Tables 1 and 3 show aqueous phase calculations with 6-311++ ( $d, p$ ) basis set and B3LYP level for molecular characteristics of compounds 1-9. It is an important parameter that can predict the chemical reactive ratio of the molecule. Consequently, the reactivity sequence for the derivatives in the liquid phase are:  $1 < 9 < 8 < 4 < 3 < 6 < 5 < 7 < 2$  liquid phase,  $1 < 9 < 8 < 3 < 4 < 5 < 6 < 7 < 2$  gas phase.

2-methyl-1, 3, 4-thiadiazole has a high hardness in the gas phase and aqueous phase, besides 2-propyl-5-methyl-1, 3, 4-thiadiazole has the lowest value of hardness. Tables 2 and 4 describe the Fukui indices which are more significant to predict the lowest and highest susceptible site for electrophilic attack. The most susceptible sites are N4 and S6. N4 and N16 have the highest amount in 2-aminoethyl-5-methyl-1, 3, 4-thiadiazole in the aqueous phase which are equal to 0.187 and 0.101. In the gas phase calculations, Cl atom in 2-(2-chloroethyl)-5-methyl-1, 3, 4-thiadiazole and N16 in 2-aminoethyl-5-methyl-1, 3, 4-thiadiazole have the maximum value of electrophilic attack which are equal to 0.125 and 0.101 respectively.

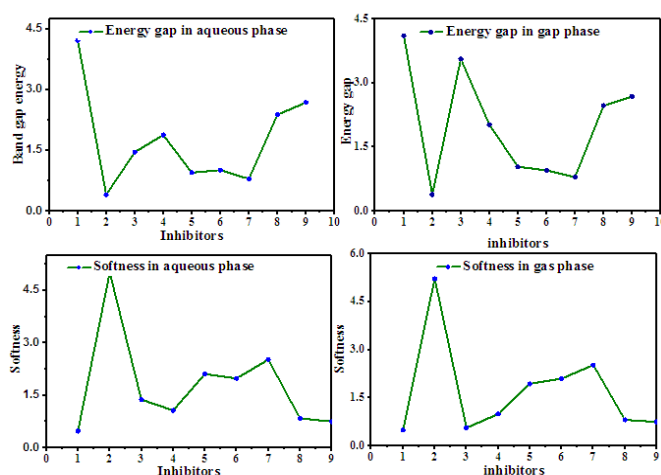


Figure 4 Variation of quantum chemical parameters with the nature of the inhibitor.

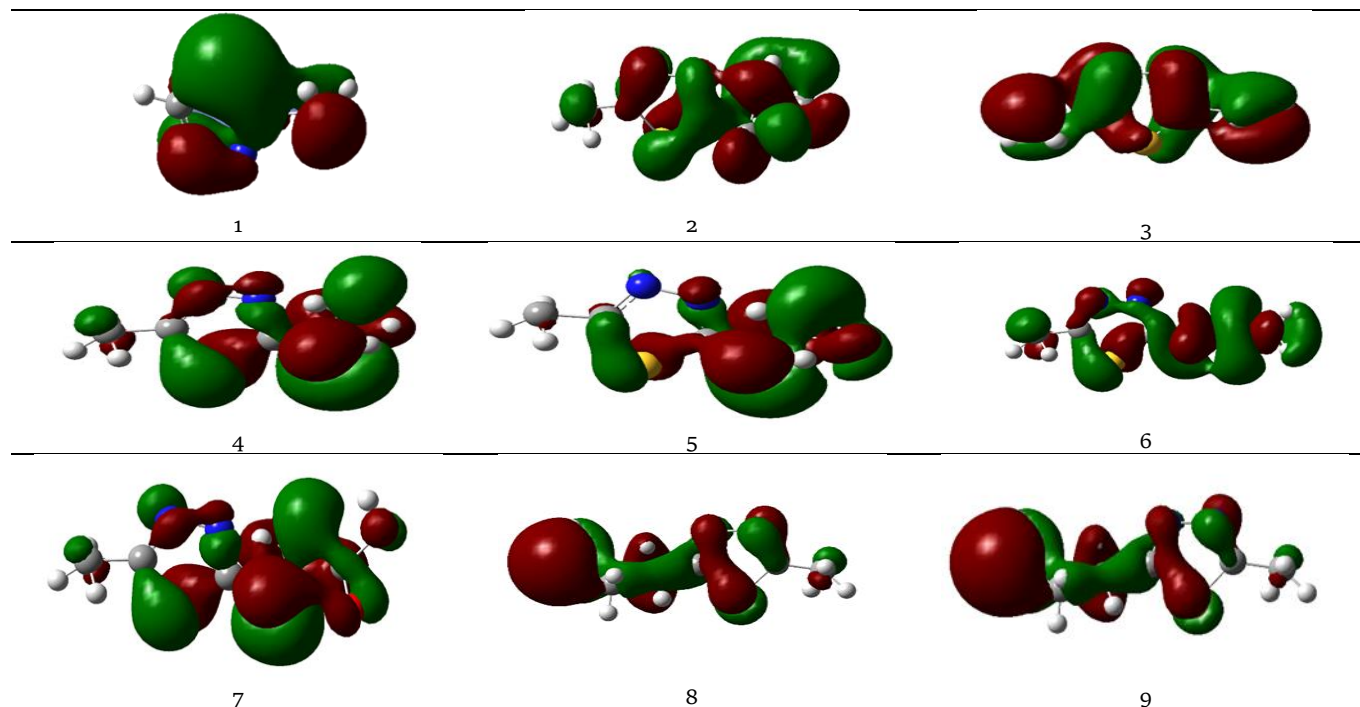


**Table 5** Quantum chemical parameters of derivatives 1–9 in the gas phase with 6-311++ (d, p) basis set and B3LYP level.

Inhibitors	1	2	3	4	5	6	7	8	9
$\Delta N$	0.674	0.843	0.456	0.212	0.310	0.183	1.244	0.257	0.642
$\Delta E_{b-d}$	-0.512	-0.047	-0.445	-0.252	-0.129	-0.119	-0.099	-0.308	-0.335

**Table 6** Quantum chemical parameters of derivatives 1–9 in the aqueous phase with 6-311++ (d, p) basis set and B3LYP level.

Inhibitors	1	2	3	4	5	6	7	8	9
$\Delta N$	0.200	-0.99	0.341	0.594	1.085	0.901	1.244	0.578	0.642
$\Delta E_{b-d}$	-0.526	-0.049	-0.18	-0.23	-0.118	-0.126	-0.099	-0.297	-0.335

**Figure 5** The optimized structures, HOMOs of non-protonated inhibitor molecules using DFT/B3LYP/6-31++G (d, p) in aqueous phase.

## 7. Conclusions

Quantum computational chemistry approach with 6-311++ (d, p) basis set and Becke's three-parameters hybrid exchange-correlation functional (B3LYP) using DFT was used to perform the theoretical calculations. We carried out the geometry optimization of the investigated compounds resulting from the substitution of the ring of 1, 3, 4-thiadiazole with various groups. HOMO and LUMO are extremely useful to determine such parameters as bandgap energy, hardness, softness, ionization energy, electrophilicity, nucleophilicity and electronegativity of molecules to indicate chemical reactive behaviour. Low bandgap and high softness indicate the interaction between inhibitor substituent and 1, 3, 4-thiadiazole. Moreover, we predicted the adsorption abilities of the 1, 3, 4-thiadiazole surface of inhibitor molecules by considering Eg and harness. In the gas phase and the aqueous phase, dynamic simulation approximations to demonstrated the corrosion inhibition performance of the studied inhibitors against the corrosion of 1, 3, 4-thiadiazole. The relative performance in the gas and aqueous phases can be given as  $1 < 9 < 8 < 3 < 4 < 5 < 6 < 7 < 2$ ,  $1 < 3 < 9 < 8 < 3 < 4 < 5 < 6 < 7 < 2$ , respectively. The Mulliken population analysis was used to

determine the Fukui indices to detect the reactive sites. In conclusion, the study shows that N4 has a more reactive site in the gaseous and aqueous phases of these derivatives. If these atoms – O, N, S – are present in the molecule, the corrosion inhibition increases. The highest value was found in the aqueous phase in the N4 atoms in 2-aminoethyl-5-methyl-1, 3, 4-thiadiazole, which has a susceptible site for electrophilic attack.

## Supplementary materials

No supplementary materials are available.

## Funding

This research had no external funding.

## Acknowledgments

None.

## Author contributions

Conceptualization: D.M.M., H.M.Q.

Data curation: D.M.M.

Formal Analysis: D.M.M., A.H.A., T.M.K.

Funding acquisition: D.M.M., H.M.Q.

Investigation: D.M.M., H.M.Q.

Methodology: D.M.M., H.M.Q.

Project administration: D.M.M.

Resources: D.M.M., H.M.Q.

Software: D.M.M.

Supervision: D.M.M.

Validation: D.M.M.

Visualization: H.M.Q.

Writing – original draft: H.M.Q., D.M.M.

Writing – review & editing: H.M.Q.

## Conflict of interest

The authors declare no conflict of interest.

## Additional information

Websites of

University of Raparin, <https://www.uor.edu.krd/en>;

Salahaddin University, <https://su.edu.krd>.

## References

- Potthast A, Henniges U, Banik G. Iron gall ink-induced corrosion of cellulose: aging, degradation and stabilization. Part 1: model paper studies. *Cellulose*. 2008;15(6):849–859. doi:[10.1007/s10570-008-9237-1](https://doi.org/10.1007/s10570-008-9237-1)
- Kim D-K, Muralidharan S, Ha T-H, Bae J-H, Ha Y-C, Lee H-G, Scantlebury J. Electrochemical studies on the alternating current corrosion of mild steel under cathodic protection condition in marine environments. *Electrochim Acta*. 2006;51(25):5259–5267. doi:[10.1016/j.electacta.2006.01.054](https://doi.org/10.1016/j.electacta.2006.01.054)
- Qadr HM. A molecular dynamics study of temperature dependence of the primary state of cascade damage processes. *Russ J Non-Ferrous Metal*. 2021;62(5):561–567. doi:[10.3103/S1067821221050096](https://doi.org/10.3103/S1067821221050096)
- Qadr HM. Pressure effects on stopping power of alpha particles in argon gas. *Phys Partic Nucl Lett*. 2021;18(2):185–189. doi:[10.1134/S1547477121020151](https://doi.org/10.1134/S1547477121020151)
- Sastri VS. *Green corrosion inhibitors: theory and practice*. John Wiley & Sons; 2012. 311 p.
- Rani B, Basu BBJ. Green inhibitors for corrosion protection of metals and alloys: an overview. *Int J Corros*. 2012;380217. doi:[10.1155/2012/380217](https://doi.org/10.1155/2012/380217)
- Sanyal B. Organic compounds as corrosion inhibitors in different environments – a review. *Prog Org Coat*. 1981;9(2):165–236. doi:[10.1016/0033-0655\(81\)80009-X](https://doi.org/10.1016/0033-0655(81)80009-X)
- Revie RW. *Corrosion and corrosion control: an introduction to corrosion science and engineering*. John Wiley & Sons; 2008. 512 p.
- Shreir LL. *Corrosion: metal/environment reactions*. Newnes; 2013. 1232 p.
- Schmitt G. Application of inhibitors for acid media: report prepared for the European federation of corrosion working party on inhibitors. *Brit Corros J*. 1984;19(4):165–176. doi:[10.1179/000705984798273100](https://doi.org/10.1179/000705984798273100)
- Obot I, Obi-Egbedi N. Theoretical study of benzimidazole and its derivatives and their potential activity as corrosion inhibitors. *Corros Sci*. 2010;52(2):657–660. doi:[10.1016/j.corsci.2009.10.017](https://doi.org/10.1016/j.corsci.2009.10.017)
- Huzinaga S, Andzelm J, Radzio-Andzelm E, Sakai Y, Tatewaki H, Klobukowski M. Gaussian basis sets for molecular calculations. Elsevier; 2012. 434 p.
- Kaya S, Kaya C, Guo L, Kandemirli F, Tüzün B, Uğurlu İ, Madkour LH, Saraçoğlu M. Quantum chemical and molecular dynamics simulation studies on inhibition performances of some thiazole and thiadiazole derivatives against corrosion of iron. *J Mol Liq*. 2016;219:497–504. doi:[10.1016/j.molliq.2016.03.042](https://doi.org/10.1016/j.molliq.2016.03.042)
- Amin MA. A newly synthesized glycine derivative to control uniform and pitting corrosion processes of Al induced by SCN<sup>-</sup> anions—Chemical, electrochemical and morphological studies. *Corros Sci*. 2010;52(10):3243–3257. doi:[10.1016/j.corsci.2010.05.041](https://doi.org/10.1016/j.corsci.2010.05.041)
- Raicheva S, Aleksiev B, Sokolova E. The effect of the chemical structure of some nitrogen-and sulphur-containing organic compounds on their corrosion inhibiting action, *Corros Sci*. 1993;34(2):343–350. doi:[10.1016/0010-938X\(93\)90011-5](https://doi.org/10.1016/0010-938X(93)90011-5)
- Growcock F. Inhibition of steel corrosion in HCl by derivatives of cinnamaldehyde: Part I. Corrosion inhibition model. *Corrosion*. 1989;45(12):1003–1007. doi:[10.5006/1.3585008](https://doi.org/10.5006/1.3585008)
- Quraishi M, Sharma HK. 4-Amino-3-butyl-5-mercapto-1, 2, 4-triazole: a new corrosion inhibitor for mild steel in sulphuric acid. *Mater Chem Phys*. 2003;78(1):18–21. doi:[10.1016/S0254-0584\(02\)00313-9](https://doi.org/10.1016/S0254-0584(02)00313-9)
- Tsuneda T. *Density functional theory in quantum chemistry*. Springer: Tokyo; 2014. doi:[10.1007/978-4-431-54825-6](https://doi.org/10.1007/978-4-431-54825-6)
- Qadr HM. Effect of ion irradiation on the mechanical properties of high and low copper. *Atom Indones*. 2020;46(1):47–51. doi:[10.17146/aij.2020.923](https://doi.org/10.17146/aij.2020.923)
- Mamand D. Theoretical calculations and spectroscopic analysis of gaussian computational examination-NMR, FTIR, UV-Visible, MEP on 2, 4, 6-Nitrophenol. *J Phys Chem Funct Mater*. 2019;2(2):77–86.
- Endredi G, Perczel A, Farkas O, McAllister M, Csonka G, Ladik J, Csizmadia I. Peptide models XV. The effect of basis set size increase and electron correlation on selected minima of the ab initio 2D-Ramachandran map of For-Gly-NH<sub>2</sub> and For-l-Ala-NH<sub>2</sub>. *J Mol Struct*. 1997;391(1–2):15–26. doi:[10.1016/S0166-1280\(96\)04695-7](https://doi.org/10.1016/S0166-1280(96)04695-7)
- Foresman J, Frish E. *Exploring chemistry*. Gaussian Inc.: Pittsburgh, USA; 1996. 304 p.
- Mineva T, Russo N. Atomic Fukui indices and orbital hardnesses of adenine, thymine, uracil, guanine and cytosine from density functional computations. *J Mol Struct*. 2010;943(1–3):71–76. doi:[10.1016/j.theochem.2009.10.023](https://doi.org/10.1016/j.theochem.2009.10.023)
- Yang W, Mortier WJ. The use of global and local molecular parameters for the analysis of the gas-phase basicity of amines. *J Am Chem Soc*. 1986;108(19):5708–5711. doi:[10.1021/ja00279a008](https://doi.org/10.1021/ja00279a008)
- Mendez F, Galván M, Garritz A, Vela A, Gàzquez J. Local softness and chemical reactivity of maleimide: nucleophilic addition. *J Mol Struct*. 1992;277:81–86. doi:[10.1016/0166-1280\(92\)87131-I](https://doi.org/10.1016/0166-1280(92)87131-I)
- Mulliken R. Electronic population analysis on LCAO–MO molecular wave functions. II. Overlap populations, bond orders, and covalent bond energies. *J Chem Phys*. 1955;23(10):1841–1846. doi:[10.1063/1.1740588](https://doi.org/10.1063/1.1740588)
- Kochi JK. Electron transfer and charge transfer: twin themes in unifying the mechanisms of organic and organometallic reactions. *Angew Chem Int Ed English* 27(10) (1988) 1227–1266. doi:[10.1002/anie.198812273](https://doi.org/10.1002/anie.198812273)
- Lee C, Yang W, Parr RG. Development of the Colle-Salvetti correlation-energy formula into a functional of the electron density. *Phys Rev B*. 1988;37(2):785. doi:[10.1103/PhysRevB.37.785](https://doi.org/10.1103/PhysRevB.37.785)
- Becke AD, Johnson ER. Exchange-hole dipole moment and the dispersion interaction. *J Chem Phys*. 2005;122(15):154104. doi:[10.1063/1.1884601](https://doi.org/10.1063/1.1884601)
- Huang Y, Rong C, Zhang R, Liu S. Evaluating frontier orbital energy and HOMO/LUMO gap with descriptors from density functional reactivity theory. *J Mol Model*. 2017;23(1):1–12. doi:[10.1007/s00894-016-3175-x](https://doi.org/10.1007/s00894-016-3175-x)
- Mamand DM, Qadr HM. Comprehensive spectroscopic and optoelectronic properties of bbl organic semiconductor. Pro-

- tect Metals Phys Chem Surf. 2021;57(5):943–953. doi:[10.1134/S207020512105018X](https://doi.org/10.1134/S207020512105018X)
32. Kavitha E, Sundaraganesan N, Sebastian S. Molecular structure, vibrational spectroscopic and HOMO, LUMO studies of 4-nitroaniline by density functional method. Indian J Pure Appl Phys. 2010;10(1):53–62.
33. Fleming I. Frontier orbitals and organic chemical reactions. New York: Wiley; 1977. 249 p.
34. Lee L-H. Correlation between Lewis acid– base surface interaction components and linear solvation energy relationship solvatochromic  $\alpha$  and  $\beta$  parameters. Langmuir. 1996;12(6):1681–1687. doi:[10.1021/la950725u](https://doi.org/10.1021/la950725u)
35. Kim K-H, Yu H, Kang H, Kang DJ, Cho C-H, Cho H-H, Oh JH, Kim BJ. Influence of intermolecular interactions of electron donating small molecules on their molecular packing and performance in organic electronic devices. J Mater Chem A. 2013;1(46):14538–14547. doi:[10.1039/C3TA13266H](https://doi.org/10.1039/C3TA13266H)
36. Elmsellem H, Harit T, Aouniti A, Malek F, Riahi A, Chetouani A, Hammouti B. Adsorption properties and inhibition of mild steel corrosion in 1 M HCl solution by some bipyrazolic derivatives: experimental and theoretical investigations. Prot Metals Phys Chem Surf. 2015;51(5):873–884. doi:[10.1134/S207020511505007X](https://doi.org/10.1134/S207020511505007X)
37. Vandewal K, Ma Z, Bergqvist J, Tang Z, Wang E, Henriksson P, Tvingstedt K, Andersson MR, Zhang F, Inganäs O. Quantification of Quantum efficiency and energy losses in low bandgap polymer: fullerene solar cells with high open-circuit voltage. Adv Funct Mater. 2012;22(16):3480–3490. doi:[10.1002/adfm.201200608](https://doi.org/10.1002/adfm.201200608)
38. Mamand D. Determination the band gap energy of poly benzimidazobenzophenanthroline and comparison between HF and DFT for three different basis sets. J Phys Chem Funct Mater. 2019;2(1):32–36.
39. Jensen WB. Overview lecture the lewis acid-base concepts: recent results and prospects for the future. J Adhes Sci Technol. 1991;5(1):1–21. doi:[10.1163/156856191X00792](https://doi.org/10.1163/156856191X00792)
40. Kabanda MM, Obot IB, Ebenso EE. Computational study of some amino acid derivatives as potential corrosion inhibitors for different metal surfaces and in different media. Int J Electrochem Sci. 2013;8:10839–10850.
41. Kaya S, Kaya C. A new equation for calculation of chemical hardness of groups and molecules. Mol Phys. 2015;113(11):1311–1319. doi:[10.1080/00268976.2014.991771](https://doi.org/10.1080/00268976.2014.991771)
42. Chakraborty T, Hens A, Kulashrestha S, Murmu NC, Banerjee P. Calculation of diffusion coefficient of long chain molecules using molecular dynamics. Phys E Low Dimens Syst Nanostruct. 2015;69:371–377. doi:[10.1016/j.physe.2015.01.008](https://doi.org/10.1016/j.physe.2015.01.008)
43. Saha SK, Hens A, RoyChowdhury A, Lohar AK, Murmu N, Banerjee P. Molecular dynamics and density functional theory study on corrosion inhibitory action of three substituted pyrazine derivatives on steel surface. Can Chem Trans. 2014;2(4):489–503. doi:[10.13179/canchemtrans.2014.02.04.0137](https://doi.org/10.13179/canchemtrans.2014.02.04.0137)
44. Özcan M, Dehri İ, Erbil M. Organic sulphur-containing compounds as corrosion inhibitors for mild steel in acidic media: correlation between inhibition efficiency and chemical structure. Appl Surf Sci. 2004;236(1–4):155–164. doi:[10.1016/j.apsusc.2004.04.017](https://doi.org/10.1016/j.apsusc.2004.04.017)
45. Bereket G, Hür E, Ögretir C. Quantum chemical studies on some imidazole derivatives as corrosion inhibitors for iron in acidic medium. J Mol Struct. 2002;578(1–3):79–88. doi:[10.1016/S0166-1280\(01\)00684-4](https://doi.org/10.1016/S0166-1280(01)00684-4)
46. Obot I, Obi-Egbedi N. Adsorption properties and inhibition of mild steel corrosion in sulphuric acid solution by ketoconazole: experimental and theoretical investigation. Corros Sci. 2010;52(1):198–204. doi:[10.1016/j.corsci.2009.09.002](https://doi.org/10.1016/j.corsci.2009.09.002)
47. Saha SK, Hens A, Murmu NC, Banerjee P. A comparative density functional theory and molecular dynamics simulation studies of the corrosion inhibitory action of two novel N-heterocyclic organic compounds along with a few others over steel surface. J Mol Liq. 2016;215:486–495. doi:[10.1016/j.molliq.2016.01.024](https://doi.org/10.1016/j.molliq.2016.01.024)
48. Cossi M, Barone V, Cammi R, Tomasi J. Ab initio study of solvated molecules: a new implementation of the polarizable continuum model. Chem Phys Lett. 1996;255(4–6):327–335. doi:[10.1016/0009-2614\(96\)00349-1](https://doi.org/10.1016/0009-2614(96)00349-1)
49. Foresman JB, Keith TA, Wiberg KB, Noonian J, Frisch MJ. Influence of cavity shape, truncation of electrostatics, and electron correlation on ab initio reaction field calculations. J Phys Chem. 1996;100(40):16098–16104. doi:[10.1021/jp960488j](https://doi.org/10.1021/jp960488j)
50. Hasanov R, Sadıkoğlu M, Bilgiç S. Electrochemical and quantum chemical studies of some Schiff bases on the corrosion of steel in H<sub>2</sub>SO<sub>4</sub> solution. Appl Surf Sci. 2007;253(8):3913–3921. doi:[10.1016/j.apsusc.2006.08.025](https://doi.org/10.1016/j.apsusc.2006.08.025)
51. Pearson RG. Absolute electronegativity and hardness correlated with molecular orbital theory. Proc Nat Acad Sci. 1986;83(22):8440–8441. doi:[10.1073/pnas.83.22.8440](https://doi.org/10.1073/pnas.83.22.8440)
52. Qadr HM, Mamand DM. Molecular structure and density functional theory investigation corrosion inhibitors of some oxadiazoles. J Bio Tribo Corros. 2021;7(4):1–8. doi:[10.1007/s40735-021-00566-9](https://doi.org/10.1007/s40735-021-00566-9)
53. Gómez B, Likhanova NV, Domínguez-Aguilar MA, Martínez-Palou R, Vela A., Gazquez JL. Quantum chemical study of the inhibitive properties of 2-pyridyl-azoles. J Phys Chem B. 2006;110(18):8928–8934. doi:[10.1021/jp057143y](https://doi.org/10.1021/jp057143y)
54. Qadr HM, Hamad AM. Using of stopping and range of ions in Matter code to study of radiation damage in materials. RENSIT. 2020;12(4):451–456. doi:[10.17725/rensit.2020.12.451](https://doi.org/10.17725/rensit.2020.12.451)